Materials Science-Poland, 40(1), 2022, pp. 1-8
http://www.materialsscience.pwr.wroc.pl/
DOI: 10.2478/msp-2022-0008

sciendo

Comparison between SEPs of $CaCO_3$ and TiO_2 in phosphor layer for better color uniformity and stable luminous flux of WLEDs with 7,000 K

Phan Xuan Le[1], Tran Thanh Trang[2], Nguyen Doan Quoc Anh[3,*], Hsiao-Yi Lee[4], Le Van Tho[5]

[1]Faculty of Mechanical – Electrical and Computer Engineering, School of Engineering and Technology, Van Lang University, Ho Chi Minh City, Vietnam

[2]Faculty of Electrical and Electronics Engineering, HCMC University of Food Industry, Ho Chi Minh City, Vietnam

[3]Faculty of Electrical and Electronics Engineering, Ton Duc Thang University, Ho Chi Minh City, Vietnam

[4]Department of Electrical Engineering, National Kaohsiung University of Science and Technology, Kaohsiung City, Taiwan

[5]Institute of Tropical Biology, Vietnam Academy of Science and Technology, Ho Chi Minh City, Vietnam

$CaCO_3$ and TiO_2 are proposed in this study as particles for scattering enhancement (SEPs) of phosphor-converted white light-emitting diodes (pc-WLEDs). The use of these two SEPs for scattering improvement enables boosting of the color homogeneity of the WLED devices. Each SEP is mixed with YAG:Ce^{3+} and silicone composition to examine their optical influences and performances on the high-power WLED packages with 7,000 K color temperature (CT). Miescattering theory is applied to calculate and investigate the scattering elements – scattering coefficients, anisotropic scattering, the reduced scattering, and scattering amplitudes – at the wavelengths of 450 nm and 550 nm. The results exhibit that TiO_2 and $CaCO_3$ considerably promote higher color uniformity and color-deviated reduction, respectively. The obtained results could be primarily attributed to the significant improvement in the scattering properties of the structure. Additionally, the effects of the presented scattering enhancement on luminous efficiency are displayed. The reduction in lumen output is observed to have a close connection with the concentration and particle size of TiO_2 and $CaCO_3$, which means that control must be exercised over these factors when utilizing these SEPs for WLED fabrication.

Keywords: *WLEDs, scattering enhancement, luminous efficiency, color quality, $CaCO_3$, TiO_2*

1. Introduction

Phosphor-converted white light-emitting diodes (pc-WLEDs), which basically contain a blue LED chip coated with a phosphor layer, usually YAG:Ce phosphor, have offered significant benefits to the lighting industry [1]. Compared to conventional light sources such as fluorescent, incandescent, mercury, and high-pressure sodium, LED can produce higher lighting efficiency that can be up to 160 lm/W [2]. Moreover, pc-LED products provide considerable energy-consumption reduction, lower maintenance costs, high resistance, long-life performance, and limitation of carbon and UV emissions [3]. Thus, LED has been gradually cementing its position in solid-state lighting (SSL) [4]. Yet, deficiencies in the color quality and the light extraction efficiency have been the obstacles preventing the phosphor-based LEDs from attaining a wider application in the SSL market [5]. In general, the phosphor-converted LED, using a YAG:Ce phosphor layer to coat the blue LED chip, generates white light by mixing the blue light from the chip that transmits through the phosphor layer with the converted yellow light produced by phosphors [6]. Particularly, a proportion of the emitted blue light is absorbed by the yellow phosphor, after which a significant amount of the resultant emitted light is yellow light. However, the yellow phosphor layer tends to absorb more scattered blue light, leading to the non-uniform color distribution. This means the yellow-light proportion is higher than that of the blue one, which probably

* E-mail: nguyendoanquocanh@tdtu.edu.vn

© Phan Xuan Le et al. 2021. This is an open access article distributed under the Creative Commons Attribution-NonCommercial-NoDerivatives 4.0 License. (http://creativecommons.org/licenses/by-nc-nd/4.0/)

results in the yellow-ring phenomenon [7, 8]. The color inconsistency can be addressed by taking advantage of the different emission characteristics of phosphor materials. In other words, combing one or more phosphor types with the yellow phosphor YAG:Ce could reduce the color deviation or the deviating correlated color temperature (D-CCT) by providing a tunable blended emission of lights [9]. Doping $Ca_9Y(PO_4)_7$ with Eu^{2+} and Sm^{3+} ions could provide the blue-green and orange-red spectral regions to the photoluminescence, which would be beneficial to the WLED that requires a high color rendering index (CRI) [10]. Another study focusing on the phosphor-in-glass structure demonstrated that the combination of silicone with other phosphor particles, including SiO_2 [11], B_2O_3 [12], PbO [13], and yellow YAG:Ce^{3+}, could minimize the color deviation by 590 K at the WLED color temperature (CT) of 6,000 K [14]. Other methods have also resulted in significant color-deviation reduction, such as HfO_2/SiO_2 DBR film providing 1,478 K reduced color differences [15] and micropatterned structure with 441 K D-CCT reduction [16] at the CT of around 5,000 K. However, the high-cost and complex production process made these methods unfavorable to the manufacturers.

The particles for scattering enhancement (SEPs) can be a more practical and potential approach for the development in color homogeneity and adequacy of WLEDs. Generally, the application of SEPs is to enhance the scattering properties of phosphor layers in the structure of LEDs, thus leading to a more uniform color distribution. The SEPs widely applied can be listed as TiO_2, $CaCO_3$, microspheres, and SiO_2 nanoparticles [17]. Besides, it is essential to ascertain the concentration and diameter of SEPs that can offer the most satisfying lighting properties. Also, it is necessary to identify the SEP that serves as the most potential material for achieving improvements in LED output and that can be applied in mass production, as well to discuss procedures by which we can carry out this identification. The paper focuses on the two SEPs of TiO_2 and $CaCO_3$ as they are frequently combined with the phosphor compound of WLED to enhance the package's lighting performance. TiO_2 particles, for example, can be mixed into the phosphor layers with the concentration of 0.1% for better color quality [18], or doped with Eu^{3+} to provide high red light emission efficiency for high-performance GaN-based WLED devices [19]. Besides, $CaCO_3$ particles have been used as a diffuser in WLED encapsulation to enhance the optical properties of the LED. It was observed that 10% $CaCO_3$ in the encapsulation showed better color uniformity while preserving the luminous-flux stability [20]. The mentioned studies on TiO_2 and $CaCO_3$ indicated the importance of the SEPs' concentration; yet the particle sizes of these particles were not thoroughly investigated. Moreover, the comparison of the performance of various SEPs by simulated scattering parameters is barely demonstrated. Hence, the present study focuses on experimenting with and analyzing the influences of TiO_2 and $CaCO_3$ via simulation and calculation of four scattering properties at the correlated color temperature (CCT) of 7,000 K. Specifically, the scattering coefficients, anisotropic scattering, the reduced scattering, and scattering amplitudes were calculated based on Mie-scattering theory [21]. A comparison between TiO_2 and $CaCO_3$ can therefore be drawn, and the most suitable SEP for WLED production can be determined. The results obtained from the present study on $CaCO_3$ and TiO_2 nanoparticles' light scattering enhancement could greatly contribute to widening the application of LEDs in other aspects, such as in biomedical fields' sensing techniques requiring high sensitivity that can be acquired by increasing the light scattered from small particles [22].

2. Scattering analysis

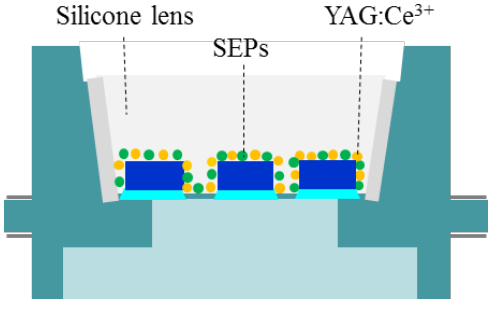
2.1. Simulated WLED model

Figure 1A presents the actual WLED used in the lighting performance investigation of TiO_2 and $CaCO_3$. In Figure 1B, the schematic illustration of this WLED is presented. Here, to simulate the required WLED, the commercial LightTools 8.1.0 (Synopsys, Inc., Mountain View, California) and the conformal phosphor coating method, which could result in better color distribution and luminous flux than other coating techniques, were ap-

plied. The multi-chip WLED package was prepared with nine LED chips attached to the lead frame by the gold wire bonding process. Given that TiO_2 and $CaCO_3$ particles are spherical, they were individually blended with the compound of yellow phosphor YAG:Ce^{3+} to form coating films with a 0.08 mm thickness, and were then placed over the LED chips' surfaces. The reflector of each WLED has a depth and inner and surface diameters of 2.1 mm, 8 mm, and 10 mm, respectively. Besides, the indices of refraction of $CaCO_3$, TiO_2, YAG:Ce^{3+} particles, and the silicone glue in visible spectral wavelengths are 1.66, 2.87, 1.83, and 1.5, respectively.



(A)



(B)

Fig. 1. **(A)** pc-LED model used in the research, **(B)** 2D schematic image of pc-LEDs model. SEPs, particles for scattering enhancement

2.2. Scattering analysis

The numeric computation of light scattering events in the LED structure was conducted with MATLAB (MathWorks, Massachusetts, USA). The theory of Mie scattering was applied to demonstrate the results of the light scattering properties in the LED, using SEPs [23]. The scattering coefficient $\mu_{sca}(\lambda)$, anisotropy factor $g(\lambda)$, and reduced scattering coefficient $\delta_{sca}(\lambda)$ of the phosphor-SEPs layer could be measured using:

$$\mu_{sca}(\lambda) = \int N(r) C_{sca}(\lambda, r) dr \tag{1}$$

$$g(\lambda) = 2\pi \int_{-1}^{1} \int p(\theta, \lambda, r) f(r) \cos\theta d\cos\theta dr \tag{2}$$

$$\delta_{sca} = \mu_{sca}(1 - g) \tag{3}$$

where $N(r)$ shows the diffusional-particle distribution density (mm^3), C_{sca} denotes the scattering crosssections (mm^2), $p(\theta, \lambda, r)$ denotes the phase function, θ indicates the scattering angle (°C), and $f(r)$ demonstrates the diffusional particles' size distribution function in the phosphor-silicone film. λ and r express the wavelength of lights (nm) and diffusional particles' radius (μm), respectively.

The $f(r)$ is calculated using:

$$f(r) = f_{dif}(r) + f_{phos}(r) \tag{4}$$

$$\begin{aligned} N(r) &= N_{dif}(r) + N_{phos}(r) \\ &= K_N \cdot \left[f_{dif}(r) + f_{phos}(r) \right] \end{aligned} \tag{5}$$

where $N_{dif}(r)$ and $N_{phos}(r)$ present the diffusional-particle and phosphorus-particle densities, respectively. $f_{dif}(r)$ indicates the diffusional-particle size distribution function, and that datum of the phosphors is represented as $f_{phos}(r)$. K_N is the diffusional-particle unit quantity for one diffusional-particle concentration, which is calculated using:

$$c = K_N \int M(r) dr \tag{6}$$

$M(r)$ – mass distribution of the diffusor unit – is expressed as follows:

$$M(r) = \frac{4}{3}\pi r^3 \left[\rho_{dif} f_{dif}(r) + \rho_{phos} f_{phos}(r) \right] \tag{7}$$

where $\rho_{diff}(r)$ indicates the density of the diffusive spheres and $\rho_{phos}(r)$ shows the density of phosphor granules.

With Mie-scattering application, C_{sca} could be shown as:

$$C_{sca} = \frac{2\pi}{k^2}\sum_{0}^{\infty}(2n-1)\left(|a_n|^2+|b_n|^2\right) \quad (8)$$

Here, $k = 2\pi/\lambda$, while a_n and b_n can be demonstrated by:

$$a_n(x,m) = \frac{\psi_n'(mx)\psi_n(x) - m\psi_n(mx)\psi_n'(x)}{\psi_n'(mx)\xi_n(x) - m\psi_n(mx)\xi_n'(x)} \quad (9)$$

$$b_n(x,m) = \frac{m\psi_n'(mx)\psi_n(x) - \psi_n(mx)\psi_n'(x)}{m\psi_n'(mx)\xi_n(x) - \psi_n(mx)\xi_n'(x)} \quad (10)$$

where $x = k \times r$, m denotes the index of refraction, and $\psi_n(x)$ and $\xi_n(x)$ indicate the Riccati–Bessel function. The computations for the relative refractive indices of diffusional sphere (m_{dif}) and phosphor grain (m_{phos}) in the silicone are: $m_{dif} = n_{dif}/n_{sil}$ and $m_{phos} = n_{phos}/n_{sil}$. Subsequently, the phase function $p(\theta,\lambda,r)$ can be reckoned using:

$$p(\theta,\lambda,r) = \frac{4\pi\beta(\theta,\lambda,r)}{k^2 C_{sca}(\lambda,r)} \quad (11)$$

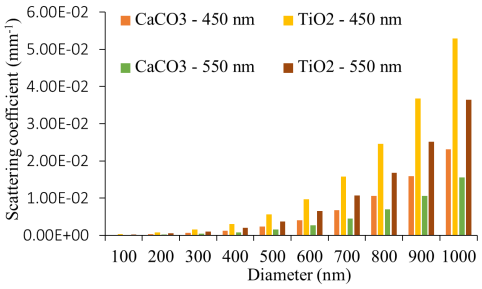
$\beta(\theta,\lambda,r)$, $S_1(\theta)$, and $S_2(\theta)$ indicate the angular scattering amplitudes, which are computed using:

$$\beta(\theta,\lambda,r) = \frac{1}{2}\left[|S_1(\theta)|^2 + |S_2(\theta)|^2\right] \quad (12)$$

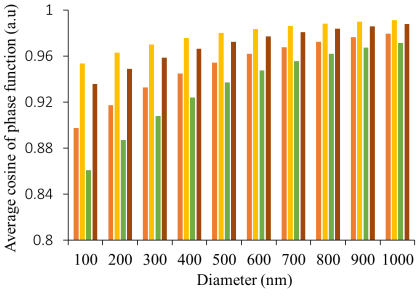
$$S_1 = \sum_{n=1}^{\infty}\frac{2n+1}{n(n+1)}\begin{bmatrix} a_n(x,m)\pi_n(\cos\theta) \\ +b_n(x,m)\tau_n(\cos\theta)\end{bmatrix} \quad (13)$$

$$S_2 = \sum_{n=1}^{\infty}\frac{2n+1}{n(n+1)}\begin{bmatrix} a_n(x,m)\tau_n(\cos\theta) \\ +b_n(x,m)\pi_n(\cos\theta)\end{bmatrix} \quad (14)$$

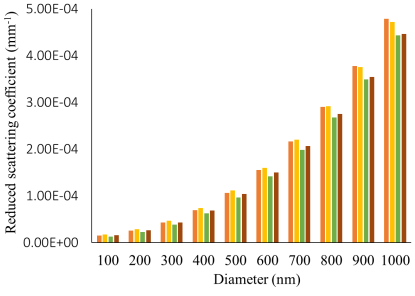
In these equations, θ is the scattering angle (°); a_n and b_n represent the expansion coefficients with even symmetry and odd symmetry, respectively; and $\pi_n(\cos\theta)$ and $\tau_n(\cos\theta)$ indicate the angular dependent functions. The computed scattering properties of $CaCO_3$ and TiO_2 at two different



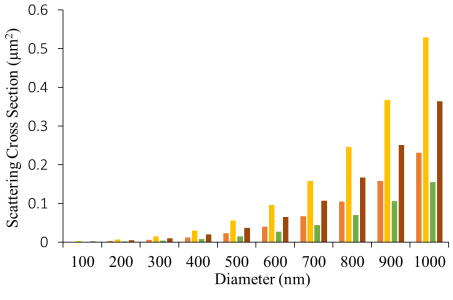
(A)



(B)



(C)



(D)

Fig. 2. Comparison of scattering properties in pc-LEDs using $CaCO_3$ and TiO_2 with different diameters at 450 nm and 550 nm: **(A)** Scattering coefficient; **(B)** Average cosine of phase function; **(C)** Reduced scattering coefficient; **(D)** Scattering cross-section

light wavelengths of 450 nm and 550 nm as a function of particle sizes are demonstrated in Figure 2. Previous studies demonstrated that a larger size of nanoparticles probably enhanced the scattering performance, while a lower size induced the adsorption cross-section to outweigh that of the scattering one, stimulating the influences of dissipation loss on the scattering factor [24]. Thus, bigger particle sizes of $CaCO_3$ and TiO_2 could be remarkably beneficial to the light scattering properties of LED packages. As can be seen from Figures 2A–2D, all the scattering characteristics of $CaCO_3$ and TiO_2 are promoted significantly as the larger SEP particles are applied. This has reinforced the point of using these two particles to achieve scattering enhancement for white LEDs. Moreover, both TiO_2 and $CaCO_3$ result in stronger blue-light scattering intensity (at 450 nm) than the intensity observed in the case of yellow light (at 550 nm), indicating that the blue light lost by absorption could be compensated, and leading to the balance in the color distribution. Additionally, the more the light scattering occurs, the more uniform the light mixing becomes. Besides, the blue-light extraction efficiency of blue rays at the right and left edges of the phosphor layer can be boosted as a result of this blue-light scattering enhancement. The extracted blue light then undergoes mixing with the extracted yellow light so as to create the yellow ring that generates white light. Consequently, the yellow ring was diminished, leading to a more adequate color quality for WLED packages. Noticeably, TiO_2 sphere produces higher scattering results than $CaCO_3$ does, and so it can be assumed that TiO_2 is more beneficial to the color distribution. However, this should be further examined to decide the most suitable SEP for better lighting performance.

The reduction in the yellow ring is advantageous to the color quality of WLED, and thus TiO_2 and $CaCO_3$ are appropriate materials for acquiring higher color distribution in the WLED. From the scattering results, it can be observed that the diameter of SEPs is important. The larger sizes of the spherical particles lead to better scattering properties. In addition to the particle size, the concentration of $CaCO_3$ and TiO_2 in the yellow phosphor layer is relevant as this could influence the particle intensity distribution in the coating film, leading to the changes in the color uniformity and luminescence of the LEDs. Generally, when the light scattering is abundant, the luminous intensity can be significantly reduced. Hence, the scattering effects of $CaCO_3$ and TiO_2 as a function of their concentrations must be analyzed and discussed in more detail, which will be presented in Section 3. Based on the findings in Section 3 and combined with the results in Section 2 concerning the calculated scattering properties of SEPs, the suitable SEP for the enhancement of the corresponding optical criteria of WLEDs is possibly determined.

3. Computation and discussion

The benefit of integrating a SEP into the original phosphor-silicone layer is the control over the particle density required to stabilize the CCT of a WLED. Particularly, with SEP, the weight percentage of each element could be balanced, thus maintaining the desired CCT, which can be expressed as follows:

$$W_{phosphor} + W_{silicone} + W_{SEP} = 100\% \qquad (15)$$

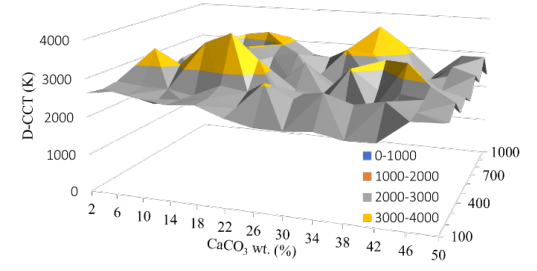
where the weight percentage of phosphor, silicone, and SEPs in the coating layer are presented as $W_{phosphor}$, $W_{silicone}$, and W_{SEP}, respectively. Based on this equation, the weight percentage of yellow phosphor YAG:Ce should decline, when the weight percentage of SEP increases as a result of the increase in its concentration, to keep the CCT stable at the determined value of 7,000 K.

The homogeneity of a WLED can be demonstrated by the extent of color deviation that occurs, which can be defined by: $\Delta CCT = CCT_{(Max)} - CCT_{(Min)}$. Here, $CCT_{(Max)}$ and $CCT_{(Min)}$ describe the maximum and minimum CCTs at the viewing angle of 0° and 90°, respectively. The color deviation, which relates to CCT variations in the light-emission angle, is the primary cause of the yellow-ring effect and the non-uniform color distribution. Previous studies pointed out that the main cause of the CCT variance is the difference between the optical properties of each element in the phosphor layer,

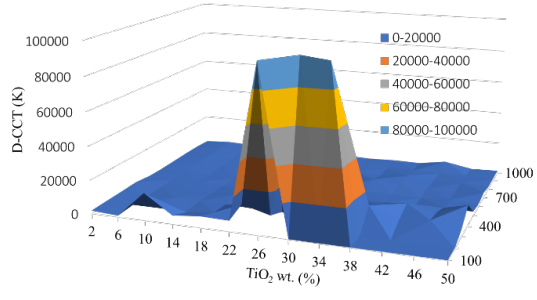
and the solution to decrease this was to increase the blue-light emission in the white-light spectra band. As the blue-light emission rises, the dissimilarity in the blue and yellow-ray proportions can be addressed. In particular, the white light is comprised of transmitted blue light and converted yellow light; therefore, to obtain the balance in these two lights, there must be enough blue-light proportions for the light transmission and light absorption to be converted into yellow light by the phosphor. When there is a shortage in the blue-light proportion essential to the yellow phosphor's absorption, most of the transmitted and scattered blue light will be absorbed and converted into yellow light. As a result, there is the apparent dominance of yellow-light proportion, causing the yellow ring on the lighting surface to appear, and consequently degrading the overall color quality. Thus, SEPs can be used as a solution to enhance the blue-light emission for a minimization in the CCT variation, which will probably result in the more homogenous chromaticity of the LED.

The CCT deviation of WLEDs with $CaCO_3$ and TiO_2 in the phosphor layer is demonstrated in Figure 3. As can be seen, both nanoparticles show remarkable performance in decreasing the variations of CCT in the light-emission angle. TiO_2 is relatively better than $CaCO_3$ in this aspect of comparison, as in Figure 3A the CCT deviation in the pc-LED with 30% TiO_2 declines two-fold, compared to that in the LED without TiO_2. Meanwhile, in Figure 3B, by using 30% $CaCO_3$ in the phosphor layer, the varied CCT decreases from 2,070 K to 1,680 K, which means there is a 390 K CCT-deviation reduction. Therefore, it is possible to use TiO_2 for enhancing the color quality of WLED; and this has confirmed the assumption mentioned in Section 2.2.

Besides the color uniformity, the luminous efficiency should also be taken into consideration as it is one of the most crucial factors in WLED quality evaluation. The lumen output of WLEDs integrat-

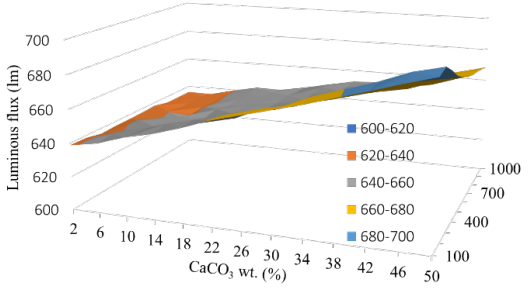


(A)

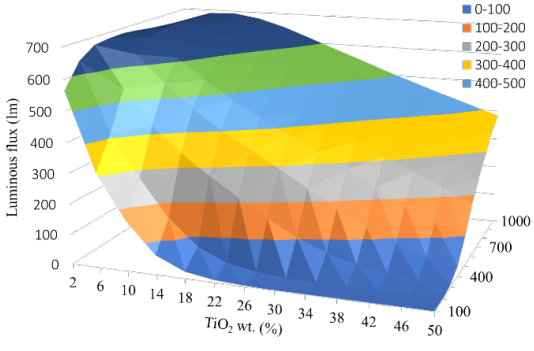


(B)

Fig. 3. The fluctuation of CCT deviation in pc-LEDs employing **(A)** $CaCO_3$ and **(B)** TiO_2. CCT, correlated color temperature



(A)



(B)

Fig. 4. Luminous flux yielded from pc-LEDs with **(A)** $CaCO_3$ and **(B)** TiO_2

ing SEPs is shown in Figure 4, in which graph (A) illustrates the luminescence of the $CaCO_3$-doped layer, and graph (B) presents that of the TiO_2-doped one. The concentrations of $CaCO_3$ and TiO_2 are adjusted in the range of 0%–50%, while their sizes range from 100 nm to 1,000 nm. As can be seen, the luminous flux declines as the concentrations of both SEPs increase. However, the luminous degradation that can be observed when there is a growth in the $CaCO_3$ concentration is much smaller than that in the case of higher TiO_2 concentrations. In other words, $CaCO_3$ can maintain the relatively high luminous stability.

To analyze the change in luminous efficiency of WLEDs using $CaCO_3$ and TiO_2, the scattering computation applying Mie theory, and the transmitted light power calculation based on Lambert-Beer law, were utilized [25]:

$$I = I_0 \exp(-\mu_{ext} L) \tag{16}$$

where I_0 and L are the incident light power and phosphor layer thickness (mm), respectively. μ_{ext} indicates the extinction coefficient, and can be defined as:

$$\mu_{ext} = N_r \cdot C_{ext}$$

where N_r denotes the number density distribution of particles (mm^{-3}) and C_{ext} (mm^2) shows the phosphor-particle extinction cross-section.

According to Eq. (16), the concentration of the SEPs is in inverse proportion to the luminous efficiency while being directly proportional to the scattering properties. In other words, the rise in SEP concentrations causes a reduction in luminescence, despite heightening the scattering occurrences in the WLED packages. Specifically, if the concentrations of $CaCO_3$ and TiO_2 continuously rise to 50wt.%, the scattering will become redundant and cause more light to be trapped, along with the increasing rate of energy loss owing to backscattering events, thus rendering the luminous flux lower. Hence, the concentration of SEPs should be managed with respect to their particle size to obtain the best results of the color and luminous performances.

4. Conclusions

The effects of two SEPs – $CaCO_3$ and TiO_2 – on the CCT uniformity and lumen efficacy are investigated, compared, and demonstrated in this article. The four scattering properties of SEPs in the phosphor layer, including the scattering coefficients, anisotropic scattering, the reduced scattering, and scattering amplitudes, are computed with Mie theory to provide a more thorough analysis of the scattering influences of $CaCO_3$ and TiO_2. The results display that both $CaCO_3$ and TiO_2 are suitable for achieving an increase in the chromatic adequacy, as they can increase the blue-light intensity to reduce the CCT variations and yellow-ring phenomenon. TiO_2 proves superior to $CaCO_3$ in stimulating the CCT-deviation reduction by presenting a two-fold lower CCT variance at a 30wt.% concentration, compared to the results at 0wt.% TiO_2. Although $CaCO_3$ resulted in a slightly lower decrease in varied CCT, by about 390 K, the luminous flux at 30% $CaCO_3$ is still higher and more stable than that at 30% TiO_2. Thus, $CaCO_3$ seems to be the better material for WLED lights, since it enables acquiring both high luminous flux and CCT homogeneity. However, it is noted that the concentrations of TiO_2 and $CaCO_3$ should be managed at a certain level to avoid the excessive scattering that induces a dramatic degradation in luminous efficacy.

Acknowledgements

This research is funded by Van Lang University, website: https://www.vanlanguni.edu.vn.

References

[1] Hanh NTM, That PT, Anh NDQ. Eu-activated strontium-barium silicate: a positive solution for improving luminous efficacy and color uniformity of white light-emitting diodes. Mater Sci Poland. 2021;38:594–600. DOI: 10.2478/msp-2020-0069.

[2] Hanh NTM, That PT, Anh NDQ, Trang TT. Triple-layer remote phosphor structure: a novel option for the enhancement of WLEDs' color quality and luminous flux. Mater Sci Poland. 2021;38:654–60. DOI: 10.2478/msp-2020-0076.

[3] That PT, Loan NTP, Tho LV, Anh NDQ, Liao HY, Luo GF, et al. Enhancing color quality of WLEDs with dual-layer remote phosphor geometry. Mater Sci Poland. 2021;38:667–4. DOI: 10.2478/msp-2020-0070.

[4] Luo GF, Loan NTP, Tho LV, Anh NDQ, Lee HY.

Enhancement of color quality and luminous flux for remote-phosphor LEDs with red-emitting $CaMgSi_2O_6$: Eu^{2+}, Mn^{2+}. Mater Sci Poland. 2020;38:409–15. DOI:10.2478/msp-2020-0045.

[5] Anh NDQ, Ngoc HV. Building superior lighting properties for WLEDs utilizing two-layered remote phosphor configurations. Mater Sci Poland. 2020;38:493–501. DOI:10.2478/msp-2020-0044.

[6] Anh NQD, Vinh NH, Lee HY. Effect of red-emitting $Sr_{2.41}F_{2.59}B_{20.03}O_{74.8}$:$Eu_{0.12}$, $Sm_{0.048}$ phosphor on color rendering index and luminous efficacy of white LEDs. Curr Opt Photon. 2017;1:118–24. DOI: 10.3807/COPP.2017.1.2.118.

[7] Anh NDQ, Vinh NH, Lee HY. Gaussian decomposition method in designing a freeform lens for an LED fishing/working lamp. Curr Opt Photon. 2017;1:233–8. DOI: 10.3807/COPP.2017.1.3.233.

[8] Jiang P, Peng Y, Mou Y, Cheng H, Chen M, Liu S. Thermally stable multi-color phosphor-in-glass bonded on flip-chip UV-LEDs for chromaticity-tunable WLEDs. Appl Opt. 2017;56:7921–6. DOI: 10.1364/AO.56.007921.

[9] Yang X, Chai C, Chen J, Zheng S, Chen C. Single 395 nm excitation warm WLED with a luminous efficiency of 104.86 lm/W and a color rendering index of 90.7. Opt Mater Express. 2019;9:4273–86. DOI: 10.1364/OME.9.004273.

[10] Yuce H, Guner T, Balci S, Demir MM. Phosphor-based white LED by various glassy particles: control over luminous efficiency. Opt Lett. 2019;44:479–82. DOI: 10.1364/OL.44.000479.

[11] Yang L, Zhang Q, Li F, Xie A, Mao L, Ma J. Thermally stable lead-free phosphor in glass enhancement performance of light emitting diodes application. Appl Opt. 2019;58:4099–104. DOI: 10.1364/AO.58.004099.

[12] Ding X, Chen Q, Tang Y, Li J, Talwar D, Yu B, et al. Improving the optical performance of multi-chip LEDs by using patterned phosphor configurations. Opt Express. 2018;26:A283–92. DOI: 10.1364/AO.58.004099.

[13] Gao W, Ding K, He G, Zhong P. Color temperature tunable phosphor-coated white LEDs with excellent photometric and colorimetric performances. Appl Opt. 2018;57:9322–7. DOI: 10.1364/AO.57.009322.

[14] Zhang J, Ji B, Hua Z. Investigations on the luminescence of $Ba_2Mg(PO_4)_2$: Eu^{2+}, Mn^{2+} phosphors for LEDs. Opt Mater Express. 2016;6:3470–5. DOI: 10.1364/OME.6.003470.

[15] Li JS, Chen YH, Li ZT, Yu SD, Tang Y, Ding XR, et al. ACU optimization of pcLEDs by combining the pulsed spray and feedback method. J Display Technol. 2016;12:1229–34. DOI: 10.1109/JDT.2016.2588419.

[16] Ge Z, Piquette A, Mishra KC, Klotzkin D. Enhanced forward emission of YAG: Ce^{3+} phosphor with polystyrene nanosphere coating. Appl Opt. 2015;54:6025–8. DOI: 10.1364/AO.54.006025.

[17] Cheng J, Zhang J, Lu J, Bian X, Zhang H, Shen Z, et al. Photoluminescence properties of $Ca_4La_6(SiO_4)_4(PO_4)_2O_2$-based phosphors for wLEDs. Chin Opt Lett. 2019;17:051602. DOI: 10.3788/COL201917.051602.

[18] Agarwal S, Haseman MS, Khamehchi A, Saadatkia P, Winarski DJ, Selim FA. Physical and optical properties of Ce: YAG nanophosphors and transparent ceramics and observation of novel luminescence phenomenon. Opt Mater Express. 2017;7:1055–65. DOI: 10.1364/OME.7.001055.

[19] Li B, Zhang D, Huang Y, Ni Z, Zhuang S. A new structure of multi-layer phosphor package of white LED with high efficiency. Chin Opt Lett. 2010;8:221–3. DOI: 10.3788/COL20100802.0221.

[20] Liu Z, Liu S, Wang K, Luo X. Measurement and numerical studies of optical properties of YAG: Ce phosphor for white light-emitting diode packaging. Appl Opt. 2010;49:247–57. DOI: 0.1364/AO.49.000247.

[21] Davis W, Ohno Y. Color quality scale. Opt Eng. 2010;49:033602. DOI: 10.1117/1.3360335.

[22] Yen WM, Weber MJ. Inorganic phosphors: compositions, preparation and optical properties. Boca Raton: CRC Press; 2004. DOI: 10.1201/9780203506325

[23] Liu S, Luo X. LED packaging for lighting applications: design, manufacturing and testing. Beijing: Chemical Industry Press and John Wiley & Sons; 2011.

[24] Fan X, Zheng W, Singh DJ. Light scattering and surface plasmons on small spherical particles. Light Sci Appl. 2014;3:1–4. DOI: 10.1038/lsa.2014.60.

[25] Tran TC, Anh ND, Loan NT. Comparison of calcium carbonate and titania particles on improving color homogeneity and luminous flux of WLEDs. Telkomnika. 2020;18:2690–5. DOI: 10.12928/telkomnika.v18i5.13552.

Received 2021-07-11
Accepted 2021-10-12